crystals

MDPI

Article

Characterization of Thermal, Ionic Conductivity and Electrochemical Properties of Some *p*-Tosylate Anions-Based Protic Ionic Compounds

Arfat Anis [1,*], Manawwer Alam [2], Abdullah Alhamidi [1], Mohammad Asif Alam [3], Ravindra Kumar Gupta [4], Mohammad Tariq [5], Hamid Shaikh [1], Anesh Manjaly Poulose [1] and Saeed M. Al-Zahrani [1]

1 SABIC Polymer Research Center (SPRC), Chemical Engineering Department, King Saud University, Riyadh 11421, Saudi Arabia; akfhk90@hotmail.com (A.A.); hamshaikh@ksu.edu.sa (H.S.); apoulose@ksu.edu.sa (A.M.P.); szahrani@ksu.edu.sa (S.M.A.-Z.)
2 Department of Chemistry, College of Science, King Saud University, Riyadh 11451, Saudi Arabia; maalam@ksu.edu.sa
3 Center of Excellence for Research in Engineering Materials (CEREM), King Saud University, Riyadh 11421, Saudi Arabia; moalam@ksu.edu.sa
4 King Abdullah Institute for Nanotechnology, King Saud University, Riyadh 11451, Saudi Arabia; rgupta@ksu.edu.sa
5 LAQV, REQUIMTE, Department of Chemistry, NOVA School of Science and Technology, NOVA University Lisbon, 2829-516 Caparica, Portugal; tariq@fct.unl.pt
* Correspondence: aarfat@ksu.edu.sa

Abstract: In the present work, six protic ionic liquid (PIL) compounds based on p-toluene sulfonic acid [PTSA] anion along with different cations viz. tetraethylenepentammonium [TEPA], triethylammonium [TEA], pyridinium [Py], N-methylpiperidinium [Pip], 1-methylimidazolium [Im], and N-methylpyrrolidinium [Pyrr] were synthesized using the standard neutralization reaction method. The structural characterization of these compounds was achieved using FTIR, ^{1}H and ^{13}C NMR spectroscopies. Thermal behavior was studied using differential scanning calorimetry to determine the melting point (T_m) and crystallization (T_c) temperatures. Thermogravimetric analysis was carried out to determine the thermal stability and degradation temperatures (Tdec) and to ascertain the hygroscopic or hydrophobic nature of the synthesized compounds. Structural effects on the outcome of various properties were witnessed and discussed in detail. Electrochemical impedance spectroscopy was utilized to study the electrical transport properties of the PILs at different temperatures. Cyclic voltammetry was performed to analyze the electrochemical stability of these PILs. Low values of activation energy indicating easy proton transportation along with good electrochemical stability make the PILs a potential candidate for use in the preparation of polymer electrolytes membranes for fuel cell applications.

Keywords: protic ionic liquids; p-toluene sulfonic acid; ionic conductivity; FTIR spectroscopy; NMR analysis

Citation: Anis, A.; Alam, M.; Alhamidi, A.; Alam, M.A.; Gupta, R.K.; Tariq, M.; Shaikh, H.; Poulose, A.M.; Al-Zahrani, S.M. Characterization of Thermal, Ionic Conductivity and Electrochemical Properties of Some *p*-Tosylate Anions-Based Protic Ionic Compounds. *Crystals* **2022**, *12*, 507. https://doi.org/10.3390/cryst12040507

Academic Editor: Dmitry Medvedev

Received: 10 March 2022
Accepted: 3 April 2022
Published: 6 April 2022

1. Introduction

Proton exchange membrane fuel cells (PEMFCs), also known as H_2/O_2 fuel cell technology, are a clean, renewable energy technology with a relatively lower environmental impact. Their high efficiency and flexibility of use on a modular basis are important advantages of H_2/O_2 fuel cells for energy production [1,2]. Nafion is currently the most widely used polymer electrolyte membrane for H_2/O_2 fuel cells because of its high proton conductivity and excellent chemical and mechanical stability. The proton conductivity of Nafion is heavily dependent on its water content, which limits its maximum operating temperature to approximately 80 °C [3,4]. Several other hydrocarbon backbone-based PEMs are employed in fuel cells, such as poly(styrene sulfonic acid), sulfonated poly(phenylene

sulfide) and sulfoarylated polybenzimidazole. Although these compounds are cheaper than Nafion, environmentally friendly (no fluorine chemistry is involved), and easy to recycle, they remain dependent on water for proton conduction [4,5]. Ideally, a polymer electrolyte for an H_2/O_2 fuel cell should be chemically and mechanically stable and display high proton conductivity without humidification at temperatures near 120 °C; these characteristics will enable superior heat and water management and increase the tolerance of the electro-catalysts to CO poisoning [6–9]. Thus, the development of a polymer electrolyte that does not rely on hydration for proton conduction has important scientific and economic potential. Proton-conducting protic ionic liquids (PILs) have recently demonstrated their potential in the development of polymer electrolyte membranes for applications in H_2/O_2 fuel cells as they do not require hydration for proton conduction.

Ionic liquids (ILs), are compounds that are solely made up of ions and have much lower melting points compared to molten salts. Due to their ionic nature, ILs exhibit high-ionic conductivity, wide electrochemical window, high thermal stability, negligible vapor pressure and good solvation capacity [10–16]. The most important aspect of ILs is their designer nature. The properties and functionality of ILs can be altered by careful selection of the combination of cation and anion. ILs are either aprotic [13–16], which indicates that they do not contain a mobile proton associated with a cation, or protic [10–12], which indicates that they contain a mobile proton associated with a cation. Aprotic ionic liquids have been successfully utilized as electrolytes in lithium-ion batteries [17] and dye-sensitized solar cells [18–21], as well as in other electrochemical devices e.g., sensors and actuators [22–24]. Protic ionic liquids (PILs) contain an active proton, which makes them suitable for application as fuel cell electrolytes. The PILs, on incorporation in a suitable polymer matrix, make the electrolyte material of choice for applications at elevated temperatures in non-humidified fuel cell systems [25–30].

To utilize ionic liquids in PEMFCs their melting point should be below 130 °C. Compared to conventional electrolytes ionic liquids-based polymer electrolytes are safer and highly thermostable with a wide operating temperature window since PILs do not evaporate readily even above 100 °C. Watanabe et al. [27] reported the operation of a hydrogen fuel cell employing anhydrous diethylmethylammonium trifluoromethanesulfonate PIL as an electrolyte which has high thermal stability (360 °C) and high ionic conductivity (4.3×10^{-2} S cm^{-1} at 120 °C). Siddique et al. [31] reported the synthesis of liquid PILs from secondary and tertiary ammonium cations with trifluoroacetate, methanesulfonate, trifluoromethanesulfonate, and tosylate anions. These salts had a high ionic conductivity value 1.4–4.9 mS cm^{-1} at 70 °C and were thermally stable up to 200–300 °C.

Keeping the potential of PILs to be used as an alternative material for fuel cell application, herein, we report the synthesis and characterization of six protic ionic liquids (PILs) based on *p*-toluene sulfonic acid [PTS] anion attached to different cations *viz*. tetraethylenepentammonium [TEPA], triethylammonium [TEA], pyridinium [Py], N-methylpiperidinium [Pip], 1-methylimidazolium [Im], and N-methylpyrrolidinium [Pyrr].

2. Experimental

2.1. Materials

p-Toluenesulfonic acid monohydrate (ACS reagent, ≥98.5%), Tetraethylenepentamine (technical grade), Triethylamine (≥99.5%) Pyridine (ACS reagent, ≥99.0%), 1-Methylimidazole (ReagentPlus®, 99%), N-Methylpiperidine (99%), and N-Methylpyrrolidine (99%) were procured from Sigma-Aldrich and were used without any further purification.

2.2. Methods

2.2.1. Synthesis of *p*-Toluene Sulfonic Acid Based Ionic Liquids

The synthesis was performed in a clean, dry two-necked round-bottomed flask equipped with a thermometer and gas inlet for purging nitrogen gas. The flask was placed in an ice bath for safety to control the heat generated during the reaction. PTSA (0.1 mol, 17.2 gm) was added carefully in small amounts using a spatula to 0.1 mol of the

base with continuous stirring over a specified period as mentioned below for each base under solvent free conditions and under a nitrogen environment. The mixture was dried for 8 h under a vacuum at 90 °C for further analysis except for TGA analysis which was performed without drying the samples to quantify the amount of water in the samples.

p-Toluenesulfonic acid monohydrate (0.1 mol, 17.2 g) and Tetraethylenepentamine (0.1 mol, 9.46 g) at 40 °C and product obtained viscous yellowish liquid at room temperature.

p-Toluenesulfonic acid (0.1 mol, 17.2 g) and Triethylamine (0.1 mol, 10.10 g) at 27 °C and the product obtained was light brown solid salt at room temperature.

p-Toluenesulfonic acid (0.1 mol, 17.2 g) and Pyridine (0.1 mol, 7.91 g) 50 °C and the product obtained was whitish solid at room temperature.

p-Toluenesulfonic acid (0.1 mol, 17.2 g) and 1-Methylimidazole (0.1 mol, 8.21 g) at 60 °C and the product obtained light yellowish semi-solid at room temperature.

p-Toluenesulfonic acid (0.1 mol, 17.2 g) and N-Methylpiperidine (0.1 mol, 9.91 g) at 80 °C and the product obtained almond color solid at room temperature.

p-Toluenesulfonic acid (0.1 mol, 17.2 g) and N-Methylpyrrolidine (0.1 mol, 8.51 g) at 80 °C and product obtained off white semi-solid at room temperature.

The structures of the synthesized protic ionic liquids (PILs) are shown in Figure 1 below.

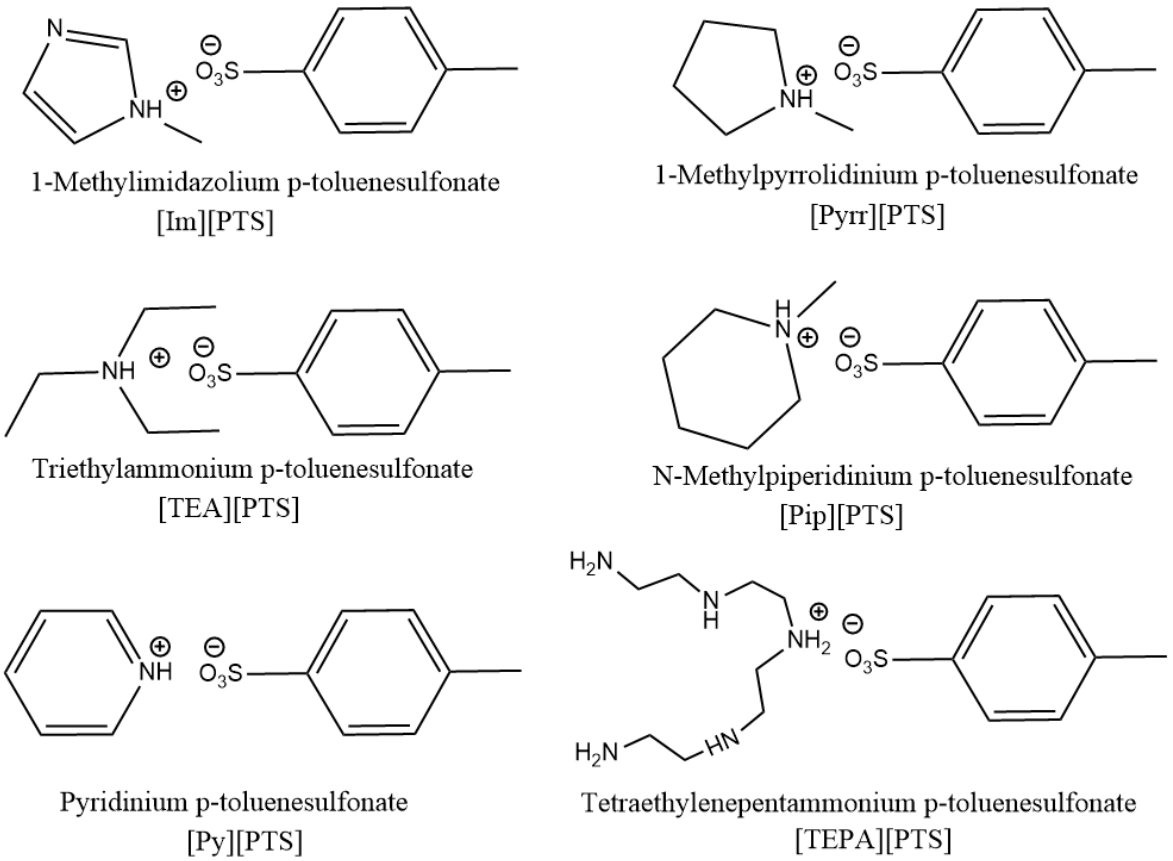

Figure 1. Structures of the 6 synthesized protic ionic liquids (PILs) based on p-toluene sulfonate anion [PTS].

2.2.2. ^{1}H and 13C NMR Analysis

Nuclear magnetic resonance (NMR) ^{1}H NMR and ^{13}C-NMR spectra were obtained for synthesized PILs using an NMR Spectrometer (JEOL DPX400MHz, Chiyoda, Tokyo, Japan). Deuterated chloroform ($CDCl_3$) was used as a solvent for the preparation of samples and tetramethylsilane (TMS) as the internal standard.

2.2.3. FTIR Spectroscopy

FTIR spectroscopy was used for vibrational characterization of all the PILs. The infrared spectrum was recorded in the frequency region of 4000–400 cm^{-1} by means of a Perkin Elmer FTIR spectrophotometer (Spectrum 100, Perkin Elmer Cetus Instrument, Norwalk, CT, USA). The analysis was performed on KBr cell window at room temperature.

2.2.4. Differential Scanning Calorimetry (DSC)

The melting and crystallization behaviors of the protic ionic liquids were examined by Differential Scanning Calorimetry (DSC-60A, Shimadzu, Tokyo, Japan). The samples were heated from an ambient temperature to 150 °C with a heating rate of 10 °C/min, then held at 150 °C for 10 min to stabilize the system and avoid drifting due to the addition of liquid nitrogen to the refrigerant reservoir; then, it was cooled to −50 °C at 10 °C/min to obtain the exothermic crystallization curve. It is again held at −50 °C for 10 min to ensure the complete removal of liquid nitrogen from the refrigerant reservoir and stabilize the system. Finally, the sample is heated again to 150 °C at 10 °C/min to obtain the melting endothermic curves in the second heating run. All measurements were performed under a nitrogen atmosphere.

2.2.5. Thermogravimetric Analysis (TGA)

The thermal stability of the ionic liquids was investigated as a function of temperature using a thermogravimetric analyzer, a Mettler Toledo AG, Analytical CH-8603 (Schwerzenbach, Switzerland). All samples (8–10 mg) were heated in alumina pan from 30 to 110 °C and held at 110 °C for 30 min to quantify the amount of water present in the samples and then the samples were finally heated up to 800 °C under. The TGA analysis was performed under argon atmosphere at flow rate of 50 mL/min using a heating rate of 10 °C/min.

2.2.6. Electrochemical Impedance Spectroscopy (EIS)

Before the measurement, the PIL was kept at ~125 °C for the whole night to remove any moisture present in the sample. The electrical conductivity (σ) was measured from 120 °C to 65 °C using the EIS. The ionic liquid was poured into a space produced by a Teflon spacer and sandwiched between platinum plates (blocking electrode), which was kept at ~125 °C [32,33]. This was subjected to 20 mV AC voltage, and real and imaginary impedances were recorded from 100 kHz to 10 Hz by a Palmsens4 Impedance Analyzer (PalmSens BV, Houten, The Netherlands). The bulk resistance (R_b) was obtained from the Nyquist plot. We estimated the electrical conductivity using the formula:

$\sigma = l/(A\ R_b)$, where l and A are the thickness and area of the PIL, respectively.

2.2.7. Cyclic Voltammetry (CV)

The cyclic voltammetry was performed by an Autolab Potentiostat (Metrohm, Amsterdam, The Netherlands) utilizing a hermetic three-electrode electrochemical cell. The potential scan rate was 0.01 V s^{-1} and the measurements were performed at different temperatures. The working, counter, and reference electrodes were made of platinum.

3. Results and Discussion

3.1. ^{1}H and ^{13}C NMR Chemical Shifts

The ^{1}H and ^{13}C NMR spectra of all the PILs are presented in Figure 2A,B, respectively along with those of the common acid, PTSA. It is evident from Figure 2A that the ^{1}H spectra shows a chemical shift relative to the pure PTSA which occurs due to the formation of the PILs by the substitution of the proton with the different cations from the respective bases used. ^{13}C NMR shown in Figure 2B also demonstrates similar chemical shifts compared to the pure PTSA. Table 1 summarizes the ^{1}H and ^{13}C NMR chemical shifts of pure PTSA along with the different PILs in $CDCl_3$. The chemical shifts reported herein agree with the ones reported elsewhere for similar protic ionic liquids [34,35].

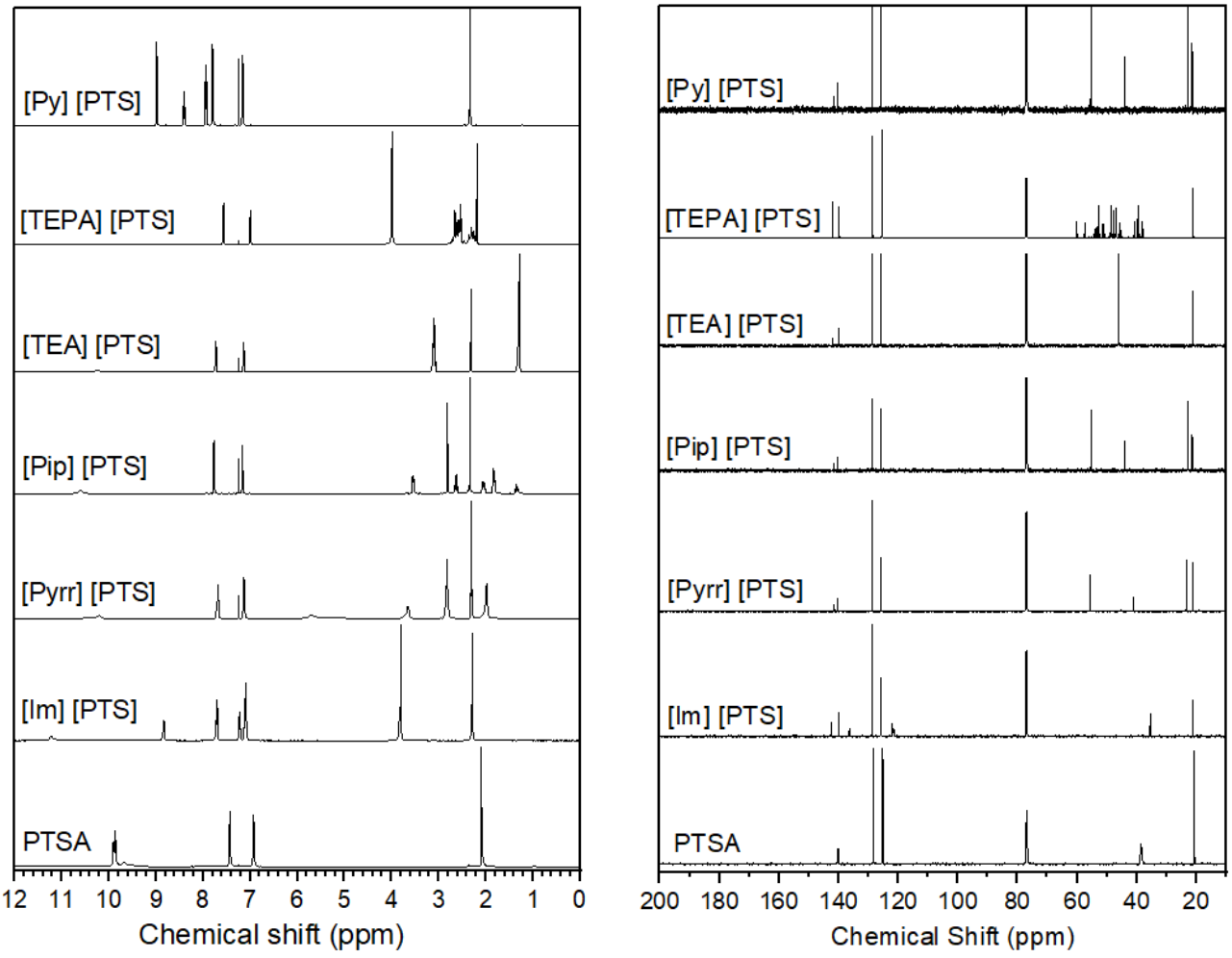

Figure 2. (**A**) ^{1}H NMR spectra of PTSA and the synthesized protic ionic liquids. (**B**) ^{13}C NMR spectra of PTSA and the synthesized protic ionic liquids.

Table 1. ^{1}H NMR and ^{13}C NMR chemical shifts of PTSA with the different cations in $CDCl_3$.

ILs	δH(ppm)			δC(ppm)				
	CH_3	CH Near CH_3	CH Near SO_3H	CH_3	C-C-SO_3^-	C-C-CH_3	C-CH_3	C-SO_3^-
PTSA	2.096	6.946	7.438	20.638	124.98	128.497	140.125	140.430
[Im][PTS]	2.302	7.128	7.698	21.220	121.410	125.722	136.319	140.020
[Pyrr][PTS]	2.321	7.130	7.673	21.239	125.760	128.868	140.373	141.603
[Pip][PTS]	2.099	7.248	7.759	21.325	125.960	128.860	140.382	141.517
[TEA][PTS]	2.311	7.140	7.718	21.268	125.855	128.726	139.962	142.223
[TEPA][PTS]	2.249	6.983	7.581	20.991	125.207	128.612	139.772	142.109
[Py][PTS]	2.329	7.150	7.784	21.325	125.960	128.860	140.373	141.546

3.2. FTIR Spectroscopy

FTIR measurements were carried out to characterize the synthesized PILs based on the interactions between the *p*-TSA and the Bronsted bases of different nature. The vibrational spectra over the whole frequency range of the PILs along with the starting components are presented in Figure 3. In PTSA, the stretching vibration of S-OH is attributed to the peak at 850 cm^{-1}, whereas the symmetric stretching and antisymmetric stretching vibration of S=O bond can be assigned to 1122 cm^{-1} and 1182 cm^{-1}, respectively. Additionally, the three oxygen atoms are equivalent in sulfonate, and various peaks can be seen in the antisymmetric stretching vibration band which appears in the spectra of the final PIL salt compounds. The sharp peak at 1182 cm^{-1} is converted to a broad peak in all the salts, and the symmetric stretching of S=O bond was found to shift from 1122 cm^{-1} to 1121 cm^{-1} [TEPA], 1128 cm^{-1} [TEA], 1124 cm^{-1} [Py], 1175cm^{-1} [Pip] 1130 cm^{-1} [Im], 1125 cm^{-1}[Pyrr], respectively. Moreover, the existence of the ionic bond N^{+}—H . . . O is indicated by the peak around 3754 cm^{-1} [36]. The N–H peaks in aliphatic amines/aromatic amines appear in the range of 3200–3100 cm^{-1} while the new broad peak at around 2230 cm^{-1} can be attributed to the interaction between the cations and the tosylate anion. The OH peak is found to red shift from 3415 cm^{-1} to 3405 cm^{-1} in the PILs indicating the presence of hydrogen bonds. All these changes indicate the formation of equimolar salts of the corresponding amines and confirm the occurrence of the acid-base neutralization reactions between the PTSA and all the amines.

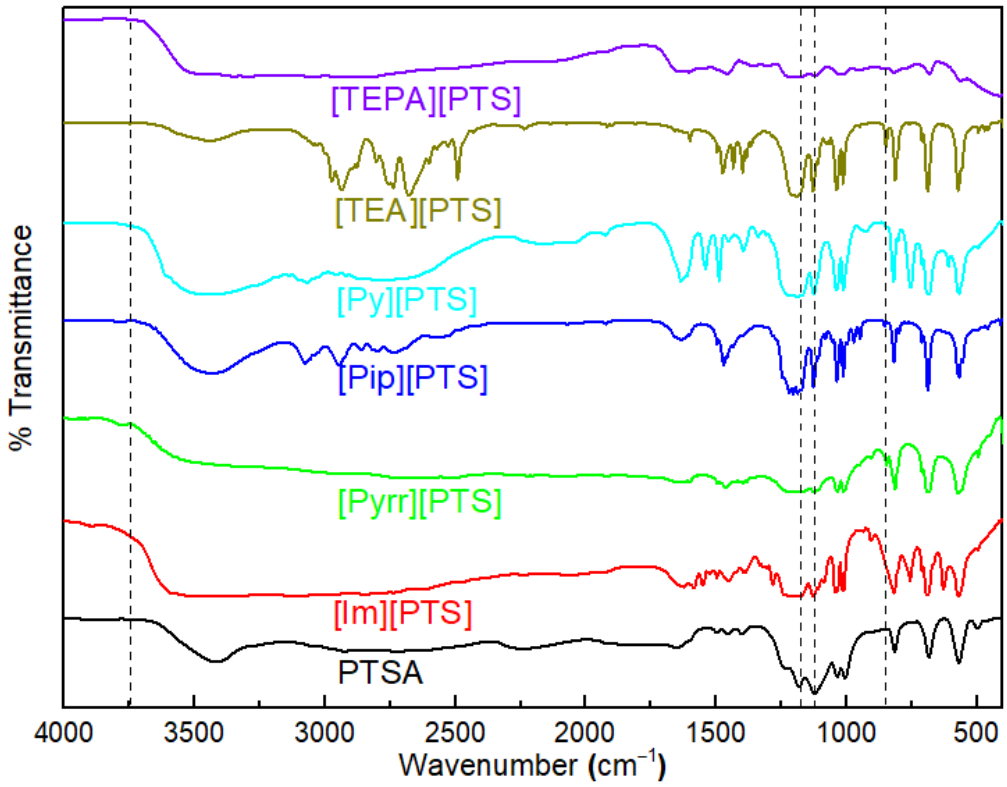

Figure 3. FTIR spectra of PTSA and the synthesized protic ionic liquids.

3.3. DSC Analysis

The melting temperature and the temperature of decomposition of the ionic liquids are the most vital properties since they determine the actual temperature range in which the ionic liquid exists in the liquid state. Many of the ionic liquids due to the incorporation of bulky ions have the tendency of super cooling and glass formation, and thus do not show any melting [37]. However, for majority of ILs, the melting point temperatures can be determined easily and accurately. There is always a possibility of minor variations in the reported melting points of the ionic liquids which occur due to various factors such

as different cooling and heating rates, sample preparation, presence of water or other impurities to name a few [38].

Technically, the crystallization temperature is the same as the melting temperature. However, for ionic liquids a considerable super cooling is observed when the ionic liquids are cooled from temperatures relatively higher than their melting temperature due to the complex packing of the ions. Figure 4 shows the DSC thermograms for the PILs. The studied protic ionic liquids show the typical PIL crystallization behavior except for the N-methyl Piperidinium *p*-toluenesulfonate which shows the crystallization peak during the heating process indicating a cold crystallization phenomenon in this particular PIL. The thermal properties of the synthesized protic ionic liquids are shown in Table 2. It should also be pointed out that the melting and crystallization peaks in the case of Tetraethylene-pentammonium *p*-toluenesulfonate were very small compared to the other PILs since it is in semi-solid form which may be due to the long aliphatic chain in the TEPA cation. The other PILs showed considerable super cooling behavior and had crystallization temperatures below 60 °C except for pyridinium *p*-toluenesulfonate which had a crystallization temperature of 74.71 °C. It can also be observed that the conductivity data of this particular PIL show an abrupt decrease/increase in conductivity due to this phase change behavior in this temperature region. It can be observed that no glass transition temperature was seen for all the PILs under the present experimental conditions.

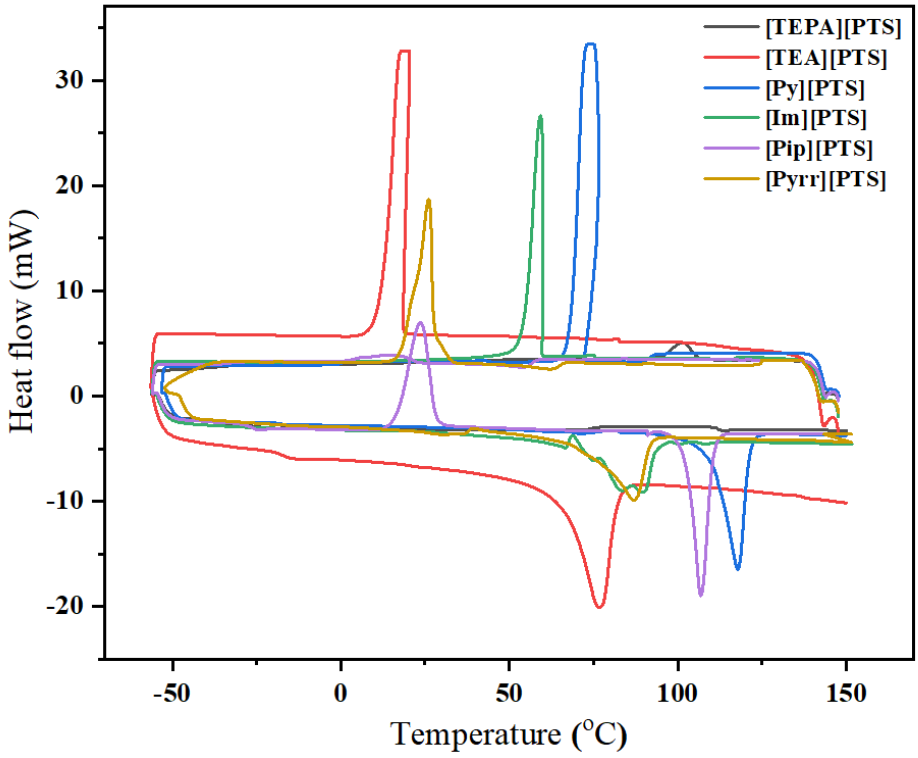

Figure 4. DSC thermogram of the *p*-toluene sulfonic acid [PTS] anion based protic ionic liquids.

Shmukler et al. [34] reported a T_m of 67.5 °C and 80.2 °C for triethylammonium *p*-toluenesulfonate with a water content of 3.4 wt. % and <1 wt. %, respectively, which is in good agreement with the T_m of 76.75 °C reported herein. The lowest T_m of 76.75 °C among the studied PILs was observed for triethylammonium *p*-toluenesulfonate, whereas the highest T_m value of 117.82 °C was observed for Pyridinium *p*-toluenesulfonate. This behavior can easily be understood by looking at the structural asymmetry in these PILs (Figure 1). Among the synthesized PILs, [TEA][PTS] has an open structure with relatively loose packing, and thus the melting is easy, whereas [Py][PTS] exhibits the most robust structure, which indicates strong packing of the ions therefore it shows an elevated melting

temperature. Since the anion, [PTS] is common for the PILs the trend observed for melting point is as follows: [Py] > [TEPA] > [Pip] > [Im] > [Pyrr] > [TEA].

Table 2. Important thermal properties of the *p*-toluene sulfonic acid [PTS] anion based protic ionic liquids (PILs).

Compound Symbol	Compound Name	T_m °C	ΔT_m (J/g)	Tc °C	ΔT_c (J/g)	T_{dec} °C
[TEPA][PTS]	Tetraethylenepentammonium *p*-toluenesulfonate	113.72	0.54	101.28	5.89	241
[TEA][PTS]	Triethylammonium *p*-toluenesulfonate	76.75	96.80	20.05	95.21	270
[Py][PTS]	Pyridinium *p*-toluenesulfonate	117.82	48.09	74.71	43.04	213
[Im][PTS]	1-Methylimidazolium *p*-toluenesulfonate	89.71	22.16	59.32	39.92	284
[Pip][PTS]	N-methyl Piperidinium *p*-toluenesulfonate	106.81	54.90	23.67	52.09	286
[Pyrr][PTS]	N-methyl Pyrrolidinium *p*-toluenesulfonate	87.12	42.61	26.01	51.38	276

T_c is the crystallization temperature; T_m is the melting temperature; T_{dec} is the decomposition temperature, stated as the temperature corresponding to a 5% loss of the sample weight.

3.4. TGA Analysis

The thermogravimetric analysis plots of the as synthesized PILs are shown in Figure 5. The thermal stability of the studied *p*-toluene sulfonate anion based ionic liquids lies within the temperature range of 225–300 °C. In order to quantify the amount of water present in the synthesized PILs the samples were held at 110 °C for an extended period to remove the water present in the samples. The water can be present in the samples due to two reasons: (i) *p*-toluenesulfonic acid monohydrate was used for their synthesis and (ii) the synthesized PILs are hygroscopic in nature. Tetraethylenepentammonium *p*-toluenesulfonate, 1-Methylimidazolium *p*-toluenesulfonate and N-methyl Pyrrolidinium *p*-toluenesulfonate shows the loss of around 3 wt. %, 4 wt. % and 7 wt. % water, respectively, from the samples as evident from the step at 110 °C showing this weight loss for these PILs. Whereas, Triethylammonium *p*-toluenesulfonate, Pyridinium *p*-toluenesulfonate and N-methyl Piperidinium *p*-toluenesulfonate samples showed almost no weight loss at 110 °C, therefore, indicating the hydrophobic nature of these 3 PILs. The remaining three PILs are hygroscopic in nature. T_{dec} is the decomposition temperature, which is the temperatures corresponding to a 5% loss in sample weight. The lowest decomposition temperature (Table 2) of 213 °C was observed for the pyridinium *p*-toluenesulfonate and the highest T_{dec} of 286 °C was observed for N-methylpiperidinium *p*-toluene sulfonate. The following trend was observed for the decomposition temperature: [Pip] > [Im] > [Pyrr] > [TEA] > [TEPA] > [Py].

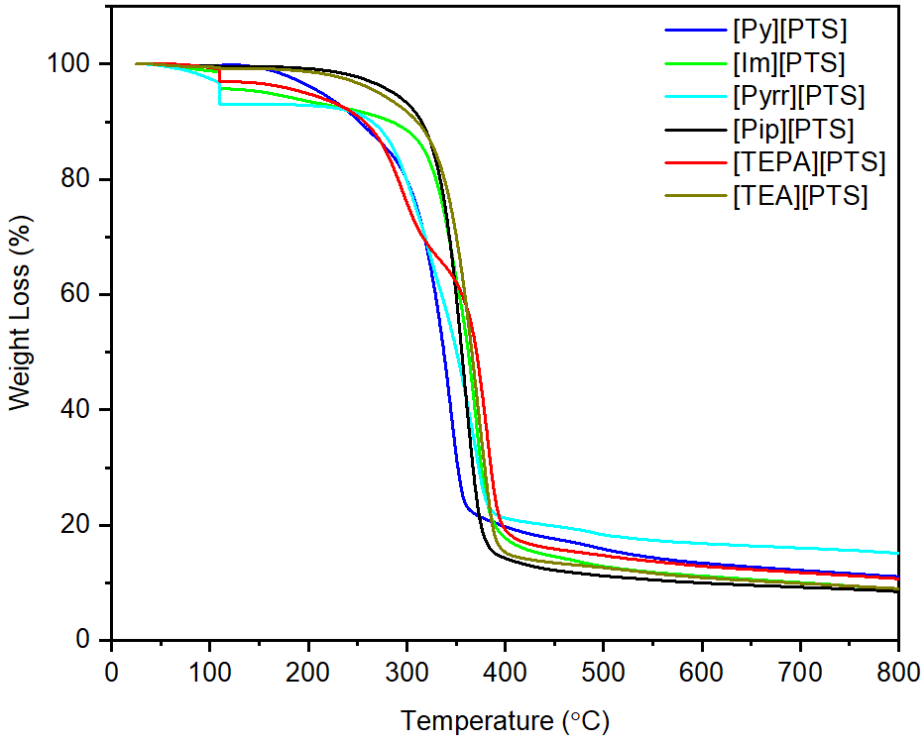

Figure 5. TGA thermogram of the *p*-toluene sulfonic acid [PTS] anion based protic ionic liquids.

3.5. Electrochemical Impedance Spectroscopy (EIS) Analysis

Figure 6 shows Nyquist plots for the PILs at ~65 °C. These plots exhibited the blocking-electrode effect in the low-frequency domain and the ionic diffusion effect in the high-frequency domain [39]. As discussed in Section 3.3, the [Py][PTS] has a crystallization temperature of 74.71 °C and due to the change in state (crystallization) below this temperature the [Py][PTS] portrayed a prominent semi-circle in the high-frequency domain at 65 °C; while the remaining PILs being in the super-cooled melt state at 65 °C exhibited the blocking-electrode effect only. As observed by Ganapatibhotla et al. [39,40] and Pires et al. [41], the super-cooled liquids have stronger cation–anion interactions. The [TEA][PTS] possessed a little change in the slope, which is probably due to a higher cation–anion interaction, as evinced by the lowest T_C peak at ~20 °C associated with this PIL. The high-frequency domain yielded the intercept at the Z'-axis, corresponding to the bulk resistance (R_b) of the PIL. Table 3 lists the evaluated σ-value for the PILs at ~65 °C. The PILs with the [TEA], [Im], [Pip], and [Pyrr] cations exhibited $\sigma_{65\,^\circ C}$-value more than 10^{-3} S cm^{-1} with the highest value of ~8.1 × 10^{-3} S cm^{-1} for the N-methyl Pyrrolidinium [Pyrr] cation, which is less than those of liquid electrolytes ($\sigma_{25\,^\circ C}$ ~10^{-2} S cm^{-1}). The conductivity of [TEA][PTS] was found here to be 2.8 × 10^{-3} at 65 °C, which is in good agreement with that reported by Shmukler et al. [34] (0.46 × 10^{-3} S cm^{-1} at 25 °C). We did not find conductivity data in the literature for the other PILs reported herein.

As mentioned earlier, the electrical conductivity was measured from 120 °C to 65 °C. Figure 7 shows log σ vs. T^{-1} plots of the PILs. The value of electrical conductivity increased with increasing temperature and formed a downward log σ vs. T^{-1} curve for all the PILs. The [Py][PTS], however, showed two conductive regions, I and II, which is due to a change in its state (crystallization) in the lower temperature region (cf. Table 2 and Section 3.3). The [Py][PTS] is in a liquid (super-cooled) state in the high-temperature region (II) and turned into solid around 75 °C (crystallization temperature) (Region I). The conductivity value was, therefore, higher in region II (liquid state) followed by a sharp drop in region I (crystallized state). Whereas for all the other PILS no such transition was observed since they existed in liquid state without any state change throughout the temperature range of conductivity measurement. The downward curves indicated the highly viscous nature of the ionic liquid

having a strong cation-anion interaction [39–41]. This type of behavior is expressed by the empirical relation: $\sigma = AT^{-1/2}\ exp[-B/k_B(T - T_o)]$ proposed by Vogel–Tamman–Fulcher (VTF), where B is the pseudo-activation energy and T_o is the temperature at which the free volume vanishes. Figure 8 shows the log $\sigma T^{1/2}$ vs. $(T - T_o)^{-1}$ plot for the PILs, which exhibited a linear trend and the slope of the linear curve resulted in a B-value. Table 3 lists the B-value for all the PILs, which are quite low, 0.028–0.079 eV. This indicated an easy transport of ions in the PILs, which is the pre-requisite for the potential usage of PILs in the preparation of polymer electrolyte for fuel cell applications.

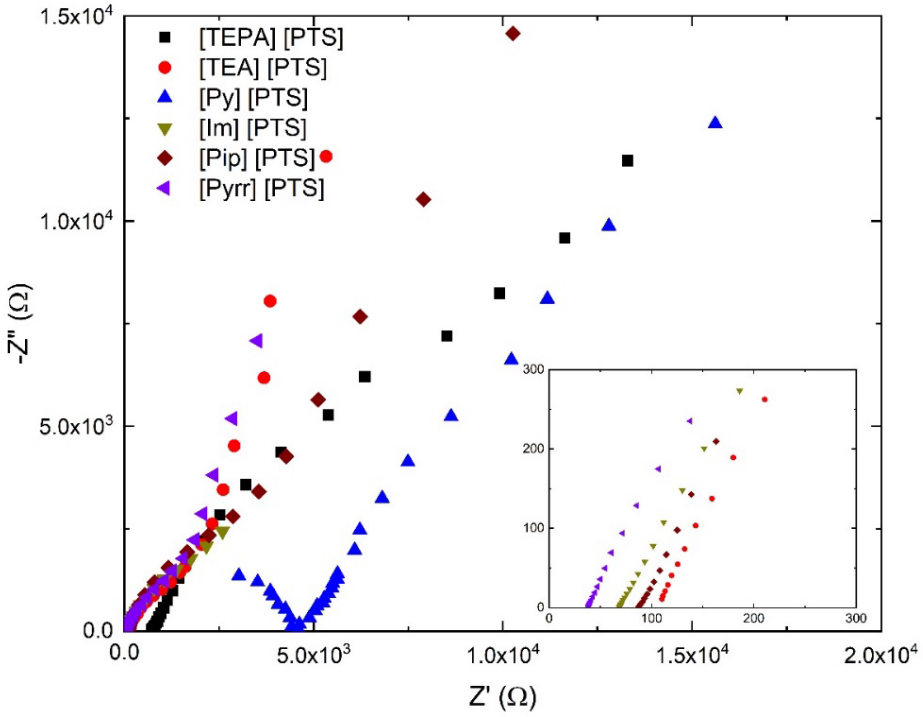

Figure 6. Nyquist plots for the ionic liquids at ~65 °C. The inset shows the high-frequency domain of some of the Nyquist plots.

Table 3. Values of electrical conductivity ($\sigma_{65\,^\circ C}$) and pseudo-activation energy (B) for the ionic liquids.

Compound Symbol	Compound Name	$\sigma_{65\,^\circ C}$ (S cm^{-1})	B (eV)
[Pyrr][PTS]	N-methyl Pyrrolidinium *p*-toluenesulfonate	8.1×10^{-3}	0.038
[Im][PTS]	1-Methylimidazolium *p*-toluenesulfonate	4.4×10^{-3}	0.028
[Pip][PTS]	N-methyl Piperidinium *p*-toluenesulfonate	3.4×10^{-3}	0.063
[TEA][PTS]	Triethylammonium *p*-toluenesulfonate	2.8×10^{-3}	0.038
[TEPA][PTS]	Tetraethylenepentammonium *p*-toluenesulfonate	4.3×10^{-4}	0.063
[Py][PTS]	Pyridinium *p*-toluenesulfonate	6.8×10^{-5}	0.079, 0.054

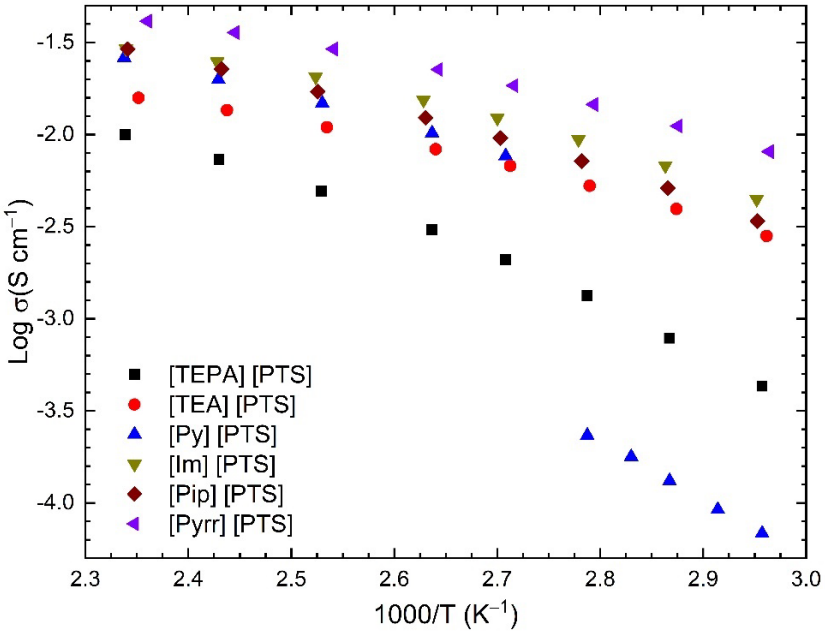

Figure 7. Log σ vs. T^{-1} plots for the PILs.

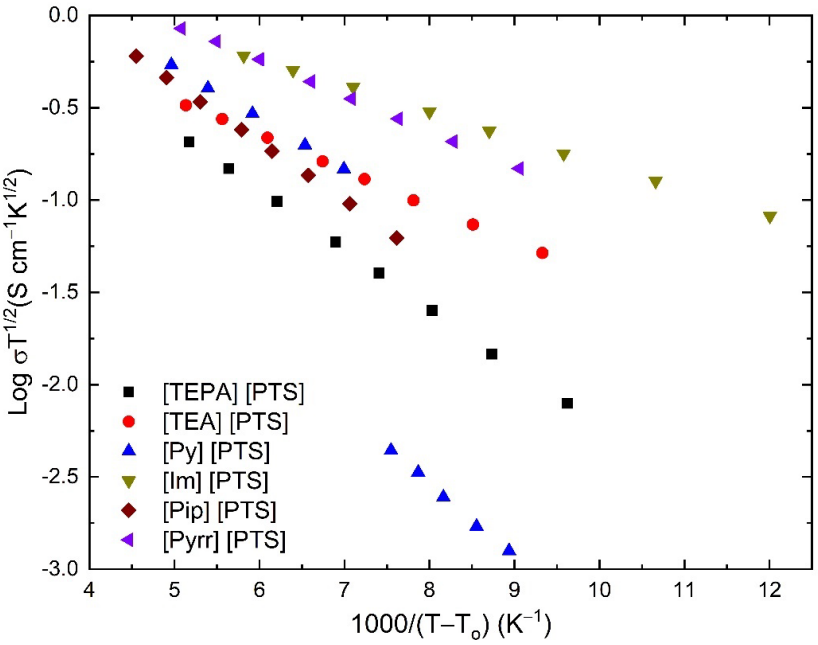

Figure 8. Log $\sigma T^{\frac{1}{2}}$ vs. $(T - T_o)^{-1}$ plots for the PILs.

3.6. Voltammetric Analysis

The electrochemical stability of the PILs depends on their electrochemical window (ECW). The electrochemical window was determined using the CV measurements. Among several factors that influence the electrochemical window of the PILs the electrode material has a considerable influence on it. The PILs being characterized here seek their potential utilization as electrolyte materials for the development of composite polymer electrolyte membranes for fuel cell application which widely uses platinum and thus platinum was used as the electrode material for the electrochemical window measurements. Generally, electrochemical characterizations are performed at elevated temperatures above the glass transition temperature of the ionic liquids, and it has been widely reported that increasing the working temperature leads to contraction of the electrochemical window of the PILs. Figure 9 shows the cyclic voltammograms of the [Pyrr][PTS] obtained at different tempera-

tures and the contraction in the ECW of the PIL is evident as reported earlier for different PILs [34,42].

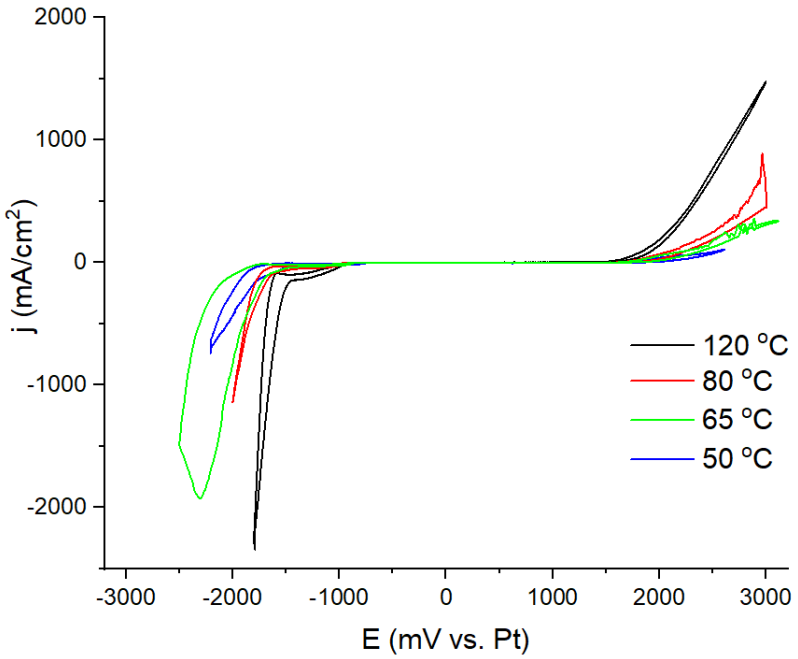

Figure 9. Cyclic voltammograms of the PIL [Pyrr][PTS] at different temperatures.

Figure 10 shows the cyclic voltammograms of PILs at 120 °C where all the PILs existed in liquid state. The voltammograms did not show any oxidation-reduction peaks, revealing good ionic properties of the abovementioned ionic liquids. The [TEA][PTS] showed the voltammogram similar to that reported earlier by Shmukler et al. [34]. The electrochemical window values of 3.1, 3.3, 2.0, 2.7, 3.1 and 3.0 V were obtained for the PILs with [TEPA], [TEA], [Py], [Im], [Pip], and [Pyrr] cations, respectively, at 120 °C.

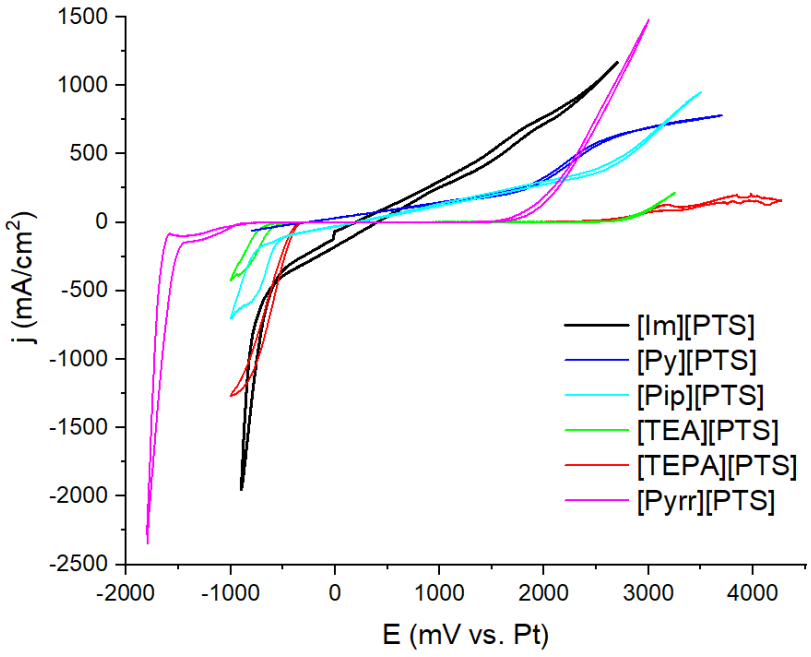

Figure 10. Cyclic voltammograms of the synthesized PILs at 120 °C.

4. Conclusions

The evaluation of the thermal and the physical properties of the prepared PILs is crucial for their potential application in electrochemical devices. PILs have enormous potential for their application in the fabrication of electrolyte membranes for fuel cell application. Six PILs based on *p*-Toluene sulfonate as anion along with structurally different bases were synthesized. The NMR and FTIR studies confirmed the formation of the PILs. Thermal characterization and phase behaviors were mapped by employing TGA and DSC studies. Impedance spectroscopy was used to evaluate their proton conductivity. The ionic conductivity for most of the synthesized salts was found to be in the range 10^{-3} S cm^{-1}. The Vogel–Tamman–Fulcher equation was used to fit the temperature dependencies of the ionic conductivity of all these PILs. The low value of activation energy (0.028–0.079 eV) indicated an easy ion transport in the ionic liquids, which is required for device applications. The low melting point along with good ionic conductivity and the electrochemical window was observed for N-methyl Pyrrolidinium *p*-toluenesulfonate and 1-Methylimidazolium *p*-toluenesulfonate. Thus, these optimal properties make these as promising PILs potential electrolytes for electrochemical applications.

Author Contributions: Conceptualization, A.A. (Arfat Anis); methodology, A.A. (Arfat Anis), M.A. and M.A.A.; formal analysis, A.A. (Arfat Anis), M.A., R.K.G., H.S. and M.T.; investigation, A.A. (Arfat Anis), M.A., A.A. (Abdullah Alhamidi) and R.K.G.; resources, A.A. (Arfat Anis), M.A. and S.M.A.-Z.; writing—original draft preparation, A.A. (Arfat Anis), M.A. and R.K.G.; writing—review and editing, A.A. (Arfat Anis), M.A.A., A.M.P., H.S., M.T. and S.M.A.-Z.; supervision, S.M.A.-Z.; funding acquisition, A.A. (Arfat Anis). All authors have read and agreed to the published version of the manuscript.

Funding: This project was funded by the National Plan for Science, Technology and Innovation (MAARIFAH), King Abdulaziz City for Science and Technology, Kingdom of Saudi Arabia, Award Number (2-17-01-001-0042).

Institutional Review Board Statement: Not applicable.

Informed Consent Statement: Not applicable.

Data Availability Statement: Data are contained within the article.

Conflicts of Interest: The authors declare no conflict of interest.

References

1. Scott, K.; Shukla, A.K. Polymer electrolyte membrane fuel cells: Principles and advances. *Rev. Environ. Sci. Bio/Technol.* **2004**, *3*, 273–280. [CrossRef]
2. Whittingham, M.S.; Savinell, R.F.; Zawodzinski, T. Introduction: Batteries and Fuel Cells. *Chem. Rev.* **2004**, *104*, 4243–4244. [CrossRef] [PubMed]
3. Muriithi, B.; Loy, D.A. Proton conductivity of Nafion/ex-situ sulfonic acid-modified stöber silica nanocomposite membranes as a function of temperature, silica particles size and surface modification. *Membranes* **2016**, *6*, 12. [CrossRef] [PubMed]
4. Rikukawa, M.; Sanui, K. Proton-conducting polymer electrolyte membranes based on hydrocarbon polymers. *Prog. Polym. Sci.* **2000**, *25*, 1463–1502. [CrossRef]
5. Aoki, M.; Chikashige, Y.; Miyatake, K.; Uchida, H.; Watanabe, M. Durability of novel sulfonated poly (arylene ether) membrane in PEFC operation. *Electrochem. Commun.* **2006**, *8*, 1412–1416. [CrossRef]
6. Myles, T.; Bonville, L.; Maric, R. Catalyst, membrane, free electrolyte challenges, and pathways to resolutions in high temperature polymer electrolyte membrane fuel cells. *Catalysts* **2017**, *7*, 16. [CrossRef]
7. Haile, S.M. Fuel cell materials and components. *Acta Mater.* **2003**, *51*, 5981–6000. [CrossRef]
8. Lee, S.-Y.; Ogawa, A.; Kanno, M.; Nakamoto, H.; Yasuda, T.; Watanabe, M. Nonhumidified intermediate temperature fuel cells using protic ionic liquids. *J. Am. Chem. Soc.* **2010**, *132*, 9764–9773. [CrossRef]
9. Li, Q.; He, R.; Jensen, J.O.; Bjerrum, N.J. Approaches and recent development of polymer electrolyte membranes for fuel cells operating above 100 C. *Chem. Mater.* **2003**, *15*, 4896–4915. [CrossRef]
10. Greaves, T.L.; Drummond, C.J. Protic ionic liquids: Properties and applications. *Chem. Rev.* **2008**, *108*, 206–237. [CrossRef]
11. Angell, C.A.; Byrne, N.; Belieres, J.-P. Parallel developments in aprotic and protic ionic liquids: Physical chemistry and applications. *Acc. Chem. Res.* **2007**, *40*, 1228–1236. [CrossRef]

12. Yoshizawa, M.; Xu, W.; Angell, C.A. Ionic liquids by proton transfer: Vapor pressure, conductivity, and the relevance of Δp K a from aqueous solutions. *J. Am. Chem. Soc.* **2003**, *125*, 15411–15419. [CrossRef]
13. Abbott, A.P.; Dalrymple, I.; Endres, F.; MacFarlane, D.R. Why use ionic liquids for electrodeposition? *Electrodepos. Ion. Liq.* **2008**, *1*, 1–15.
14. Freemantle, M. *An introduction to ionic liquids*; Royal Society of Chemistry Publishing: Cambridge, UK, 2010.
15. Rogers, R.; Plechkova, N.; Seddon, K. Ionic liquids: From knowledge to application. In *Proceedings of ACS Symposium Series*; ACS Publications: Washington, DC, USA, 2009.
16. Wasserscheid, P.; Welton, T. *Ionic Liquids in Synthesis*; WILEY-VCH Verlag GmbH & Co. KGaA: Weinheim, Germany.
17. Lewandowski, A.; Świderska-Mocek, A. Ionic liquids as electrolytes for Li-ion batteries—An overview of electrochemical studies. *J. Power Sources* **2009**, *194*, 601–609. [CrossRef]
18. Pringle, J.M.; Armel, V. The influence of ionic liquid and plastic crystal electrolytes on the photovoltaic characteristics of dye-sensitised solar cells. *Int. Rev. Phys. Chem.* **2011**, *30*, 371–407. [CrossRef]
19. Shi, D.; Pootrakulchote, N.; Li, R.; Guo, J.; Wang, Y.; Zakeeruddin, S.M.; Grätzel, M.; Wang, P. New Efficiency Records for Stable Dye-Sensitized Solar Cells with Low-Volatility and Ionic Liquid Electrolytes. *J. Phys. Chem. C* **2008**, *112*, 17046. [CrossRef]
20. Thorsmølle, V.K.; Rothenberger, G.; Topgaard, D.; Brauer, J.C.; Kuang, D.-B.; Zakeeruddin, S.M.; Lindman, B.; Grätzel, M.; Moser, J.-E. Extraordinarily efficient conduction in a redox-active ionic liquid. *arXiv* **2010**, arXiv:1011.2182. [CrossRef]
21. Armel, V.; Pringle, J.M.; Forsyth, M.; MacFarlane, D.R.; Officer, D.L.; Wagner, P. Ionic liquid electrolyte porphyrin dye sensitised solar cells. *Chem. Commun.* **2010**, *46*, 3146–3148. [CrossRef]
22. Abraham, T.J.; MacFarlane, D.R.; Pringle, J.M. Seebeck coefficients in ionic liquids–prospects for thermo-electrochemical cells. *Chem. Commun.* **2011**, *47*, 6260–6262. [CrossRef]
23. Fernandes, L.C.; Correia, D.M.; Fernández, E.; Tariq, M.; Esperança, J.M.S.S.; Lanceros-Méndez, S. Design of Ionic-Liquid-Based Hybrid Polymer Materials with a Magnetoactive and Electroactive Multifunctional Response. *ACS Appl. Mater. Interfaces* **2020**, *12*, 42089–42098. [CrossRef]
24. Correia, D.M.; Martins, P.; Tariq, M.; Esperança, J.M.S.S.; Lanceros-Méndez, S. Low-field giant magneto-ionic response in polymer-based nanocomposites. *Nanoscale* **2018**, *10*, 15747–15754. [CrossRef]
25. Lu, J.; Yan, F.; Texter, J. Advanced applications of ionic liquids in polymer science. *Prog. Polym. Sci.* **2009**, *34*, 431–448. [CrossRef]
26. Ogihara, W.; Kosukegawa, H.; Ohno, H. Proton-conducting ionic liquids based upon multivalent anions and alkylimidazolium cations. *Chem. Commun.* **2006**, 3637–3639. [CrossRef]
27. Nakamoto, H.; Watanabe, M. Brønsted acid–base ionic liquids for fuel cell electrolytes. *Chem. Commun.* **2007**, 2539–2541. [CrossRef]
28. Susan, M.A.; Noda, A.; Mitsushima, S.; Watanabe, M. Brønsted acid–base ionic liquids and their use as new materials for anhydrous proton conductors. *Chem. Commun.* **2003**, 938–939. [CrossRef]
29. Nakamoto, H.; Noda, A.; Hayamizu, K.; Hayashi, S.; Hamaguchi, H.-o.; Watanabe, M. Proton-Conducting properties of a brønsted Acid−Base ionic liquid and ionic melts consisting of bis (trifluoromethanesulfonyl) imide and benzimidazole for fuel cell electrolytes. *J. Phys. Chem. C* **2007**, *111*, 1541–1548. [CrossRef]
30. Fernicola, A.; Scrosati, B.; Ohno, H. Potentialities of ionic liquids as new electrolyte media in advanced electrochemical devices. *Ionics* **2006**, *12*, 95–102. [CrossRef]
31. Siddique, T.; Balamurugan, S.; Said, S.; Sairi, N.; Normazlan, W. Synthesis and characterization of protic ionic liquids as thermoelectrochemical materials. *RSC Adv.* **2016**, *6*, 18266–18278. [CrossRef]
32. Gupta, R.K.; Bedja, I.; Islam, A.; Shaikh, H. Electrical, structural, and thermal properties of succinonitrile-LiI-I-2 redox-mediator. *Solid State Ion.* **2018**, *326*, 166–172. [CrossRef]
33. Gupta, R.K.; Shaikh, H.; Bedja, I. Understanding the Electrical Transport–Structure Relationship and Photovoltaic Properties of a [Succinonitrile–Ionic Liquid]–LiI–I2 Redox Electrolyte. *ACS Omega* **2020**, *5*, 12346–12354. [CrossRef]
34. Shmukler, L.E.; Gruzdev, M.S.; Kudryakova, N.O.; Fadeeva, Y.A.; Kolker, A.M.; Safonova, L.P. Thermal behavior and electrochemistry of protic ionic liquids based on triethylamine with different acids. *RSC Adv.* **2016**, *6*, 109664–109671. [CrossRef]
35. Gao, G.; Zhao, Q.; Yang, C.; Jiang, T. p-Toluenesulfonic acid functionalized imidazole ionic liquids encapsulated into bismuth SBA-16 as high-efficiency catalysts for Friedel–Crafts acylation reaction. *Dalton Trans.* **2021**, *50*, 5871–5882. [CrossRef] [PubMed]
36. Miyan, L.; Qamar, S.; Ahmad, A. Synthesis, characterization and spectrophotometric studies of charge transfer interaction between donor imidazole and π acceptor 2,4-dinitro-1-naphthol in various polar solvents. *J. Mol. Liq.* **2017**, *225*, 713–722. [CrossRef]
37. Esperança, J.M.S.S.; Tariq, M.; Pereiro, A.B.; Araújo, J.M.M.; Seddon, K.R.; Rebelo, L.P.N. Anomalous and Not-So-Common Behavior in Common Ionic Liquids and Ionic Liquid-Containing Systems. *Front. Chem.* **2019**, *7*, 450. [CrossRef] [PubMed]
38. Aguirre, C.L.; Cisternas, L.A.; Valderrama, J.O. Melting-Point Estimation of Ionic Liquids by a Group Contribution Method. *Int. J. Thermophys.* **2012**, *33*, 34–46. [CrossRef]
39. Ganapatibhotla, L.V.N.R.; Wu, L.; Zheng, J.; Jia, X.; Roy, D.; McLaughlin, J.B.; Krishnan, S. Ionic liquids with fluorinated block-oligomer tails: Influence of self-assembly on transport properties. *J. Mater. Chem.* **2011**, *48*, 19275–19285. [CrossRef]
40. Ganapatibhotla, L.V.N.R.; Zheng, J.; Roy, D.; Krishnan, S. PEGylated Imidazolium Ionic Liquid Electrolytes: Thermophysical and Electrochemical Properties. *Chem. Mater.* **2010**, *22*, 6347–6360. [CrossRef]

41. Pires, J.; Timperman, L.; Jacquemin, J.; Balducci, A.; Anouti, M. Density, conductivity, viscosity, and excess properties of (pyrrolidinium nitrate-based Protic Ionic Liquid+propylene carbonate) binary mixture. *J. Chem. Thermodyn.* **2013**, *59*, 10–19. [CrossRef]
42. Shmukler, L.E.; Gruzdev, M.S.; Kudryakova, N.O.; Fadeeva, Y.A.; Kolker, A.M.; Safonova, L.P. Triethylammonium-based protic ionic liquids with sulfonic acids: Phase behavior and electrochemistry. *J. Mol. Liq.* **2018**, *266*, 139–146. [CrossRef]